Influence of Exit Geometry in Circulating Fluidized-Bed Risers

A. T. Harris and J. F. Davidson
Dept. of Chemical Engineering, University of Cambridge, Cambridge, CB2 1RA, UK

R. B. Thorpe
Dept. of Chemical & Process Engineering, University of Surrey, Surrey, GU2 7XH, UK

The influence of exit geometry on the riser axial pressure profile in circulating fluidized beds (CFB) is examined. Experiments were performed in an academic-scale CFB operating at conditions chosen to give dimensional similarity with an industrial CFB combustor. The influence of riser exit geometry was investigated to compare smooth and abrupt exits in terms of three different measures: (1) a dimensionless length of influence, Ω, of the exit along the riser, where Ω = (length of influence)/(riser height); (2) the exit reflection coefficient, R_f, defined by Senior in 1992 where R_f = (downward solids flow in riser)/(upward solids flow in riser) just below the riser exit; and (3) the increase in cross-sectionally averaged solids concentration at the riser exit. Analysis of the new data and results from the literature, lead to the description of solids flow at the exit in terms of a riser exit Froude number (Fr_R) where $Fr_R = u_{st}/gR$. A correlation between the riser exit Froude number and the exit reflection coefficient is presented. A serious correlation between the dimensionless length of influence of the exit bend, measured down the riser, and operating conditions, particle properties, gas properties and riser dimensions is also presented. Both correlations predict the influence of exit geometry (the exit effect) on the riser axial pressure profile. The relationship between operating parameters and the increase in cross-sectional averaged solids concentration at the riser exit is also examined.

Introduction

The hydrodynamics of circulating fluidized-bed (CFB) risers are highly complex. In order to understand these flow patterns better, a large volume of work has been conducted in the past two decades, with the ultimate aim of improving the performance of the CFB in industrial situations. The type and configuration of the exit used at the top of a CFB can have a significant impact upon the riser hydrodynamics, particularly in industrial-scale units. It is the aim of this work to quantify these effects in an experimental CFB with similarity to an industrial unit.

A large number of studies have examined the influence of exit geometry in circulating fluidized beds. These studies include experiments performed in cold, laboratory-scale units (of circular and square cross section) and FCC risers. No attempts to examine the influence of exit geometry in full-scale CFB combustors have been made, presumably because the cost of varying the riser exit for this type of equipment would be prohibitive.

Despite the large volume of published work, there remains one key ambiguity. What factors influence how far down the riser the effect of the exit extends? This clearly has critical implications for operators and designers. The type of exit used, its internal configuration (such as baffled or unbaffled), the size of the capped extension at the top of the bend, and the relative cross-sectional area of the exit inlet and outlet can have a dramatic effect on the internal recycling of solids in a riser, and subsequently on the riser hydrodynamics and particle residence-time distribution.

The purpose of this communication is to clarify the influence of exit geometry on the riser axial solids concentration profile and draw together the experimental data published to date.

Correspondence concerning this article should be addressed to A. T. Harris.

Previous studies of the influence of riser exit are listed in Table 1. With the exception of Martin et al. (1992b), all were performed in cold-model, laboratory-scale units. The majority of experiments were performed in risers with a circular cross section.

In general, two types of exit were studied: a smooth, "once through" exit and an abrupt, "internal reflux" exit [see, for example, Werther and Hirschberg (1997) and Grace (1990)]. The once-through exit is smoothly curved and allows for large net solids operating fluxes. These exits are likely to be used when short, uniform particle residence times are required (Grace, 1990). Abrupt exits usually consist of a 90° bend that is sometimes capped with an extension (that is, the riser extends above the outlet of the riser). This arrangement can cause significant internal refluxing of solids. van der Meer (1997) described thirteen further variations of riser exit discussed in the literature.

A number of investigators have reported apparently conflicting results concerning the influence of the riser exit.

Reviews by Horio (1997), Werther and Hirschberg (1997), and Lim et al. (1995) concluded that the exit design can affect the density profile over several meters in the upper re-

Table 1. Studies Reporting the Influence of Riser Exit on a CFB Riser

Author	Unit	Particles	Particle Properties	Operating Conditions	Riser Dimensions	Exit Type
Bai et al. (1992)	Lab. riser (circular c.s.)	FCC	$d_p = 54\ \mu$m $\rho_p = 1{,}545$ kg/m^3 $U_t^* = 0.13$ m/s	$G_s = 35$–140 kg/m^2·s $U_g = 4.33$–7.04 m/s	$D = 0.140$ m $H = 10$ m	Right-angle air-cushion bend (abrupt). Right-angle bend with 45° guiding baffle (smooth)
Brereton (1987)	Lab. riser (circular c.s.)	Sand	$d_p = 177\ \mu$m $\rho_p = 2{,}650$ kg/m^3 $U_t^* = 1.27$ m/s	$G_s = 73$ kg/m^2·s $U_g = 7.1$ m/s	$D = 0.152$ m $H = 9.3$ m	Smooth and abrupt exits
Brereton and Grace (1994)	Lab. riser (circular c.s.)	Sand	$d_p = 177\ \mu$m $\rho_p = 2{,}650$ kg/m^3 $U_t^* = 1.27$ m/s	$G_s = 9$–89 kg/m^2·s $U_g = 3.7$–9.2 m/s	$D = 0.152$ m $H = 9.3$ m	Abrupt, extended abrupt and smooth exits
Jin and Zheng (1996)	Lab. riser (square c.s.)	Resin	$d_p = 500\ \mu$m $\rho_p = 1{,}400$ kg/m^3	$G_s = 4.24$–10.3 kg/m^2·s $U_g = 5.14$ m/s	$D = 0.9 \times 0.9$ m^2 $H = 5.3$ m	Reduced outlet diameter exits with variable-length internal nose
Jin et al. (1988)	Lab. riser (circular c.s.)	FCC Silica gel	$d_p = 59\ \mu$m $\rho_p = 1{,}545$ kg/m^3 $U_t^* = 0.15$ m/s $d_p = 165\ \mu$m $\rho_p = 711$ kg/m^3 $U_t^* = 0.41$ m/s	$G_s = 30$–180 kg/m^2·s $U_g = 1.3$–10 m/s	$D = 0.14$ m $H = 11$ m	Right-angle air-cushion bend (abrupt). Right-angle bend with 45° guiding baffle (smooth)
Johnsson et al. (1999)	Lab. riser (square c.s.)	Steel Iron	$d_p = 46\ \mu$m $\rho_p = 8{,}027$ kg/m^3 $d_p = 55\ \mu$m $\rho_p = 7{,}860$ kg/m^3	$G_s = 0.05$–50 kg/m^2·s $U_g = 0.5$–5 m/s	$D =$ n/a m $H =$ n/a m	Abrupt, capped abrupt, and extended capped abrupt. Various baffles and inserts
Martin et al. (1992a)	Lab. riser (circular c.s.)	FCC	Not given	$G_s = 124$–216 kg/m^2·s $U_g = 5.2$ m/s	$D = 0.19$ m $H = 11.4$ m	Blind-T exit
Martin et al. (1992b)	FCC riser (circular c.s.)	FCC	Not given	$G_s = 298$–325 kg/m^2·s $U_g = 11.3$–14.2 m/s	$D = 0.94$ m $H = 27$ m	Blind-T exit
Mickal et al. (2001)	Lab. riser (circular c.s.)	Not given	$d_p = 20\ \mu$m $\rho_p = 2{,}150$ kg/m^3	$G_s = 0.38$–0.76 kg solid/kg gas $U_g = 2.35$–3.3 m/s	$D = 0.2$ m $H = 3.66$ m	Blind-T exit, with different capped extensions
Pugsley et al. (1997)	Lab. riser (circular c.s.)	Sand	$d_p = 220\ \mu$m $d_p = 230\ \mu$m $\rho_p = 2{,}500$ kg/m^3 $\rho_p = 2{,}600$ kg/m^3 $U_t^* = 1.73$ m/s	$G_s = 10$–45 kg/m^2·s $U_g = 4$–6 m/s	$D = 0.1$ m, 0.2 m $H = 6$ m, 12 m	Smooth and abrupt exits
Pugsley et al. (1997)	Lab. riser (circular c.s.)	FCC	$d_p = 71\ \mu$m $d_p = 80\ \mu$m $\rho_p = 2{,}200$ kg/m^3 $\rho_p = 1{,}500$ kg/m^3 $U_t^* = 0.26$ m/s	$G_s = 10$–85 kg/m^2·s $U_g = 4$–6 m/s	$D = 0.1$ m, 0.2 m $H = 6$ m, 12 m	Smooth and abrupt exits
van der Meer et al. (2000)	Lab. riser (square c.s.)	FCC	$d_p = 48\ \mu$m $\rho_p = 1{,}700$ kg/m^3 $U_t^* = 0.13$ m/s	$G_s = 1$–5 kg/m^2·s $U_g = 1$–3 m/s	$D = 0.14 \times 0.14$ m^2 $H = 5$ m	Seven different exit bends (smooth and abrupt)
Zheng and Zhang (1994)	Lab. riser (circular c.s.)	Resin	$d_p = 550\ \mu$m $\rho_p = 1{,}400$ kg/m^3 $U_t^* = 2.78$ m/s	$G_s = 4.16$–31.6 kg/m^2·s $U_g = 5.2$–6.24 m/s	$D = 0.102$ m $H = 5.25$ m	Right-angle air-cushion bend —no extension (abrupt). Right-angle air-cushion bend —variable extension (abrupt) Right-angle air-cushion bend with 45° guiding baffle (smooth)

*Single-particle terminal velocity in air.

gion of a riser. Lim et al. also noted that a strong exit restriction gives a C-shaped solids concentration profile, while a weak exit restriction does not. These conclusions are in agreement with those of Martin et al. (1992a, 1992b), who performed experiments in both laboratory- and industrial-scale FCC risers. Zheng and Zhang (1994) and Bai et al. (1992) found that abrupt exits influence only the upper portion of a riser, while smooth exits show little influence at all on the pressure profile. Zheng and Zhang (1994) also investigated the influence of a capped extension on the riser pressure profile. Their results indicated that the length of the capped extension at the top of an abrupt exit can increase the pressure drop over the exit considerably.

At the University of British Columbia (UBC), Brereton (1987) and subsequently Senior (1992) investigated the differences in apparent solids suspension density in risers with smooth and abrupt exits. They concluded that abrupt exits internally reflect a substantial portion of the arriving core solids down the riser wall, while smooth exits allow the majority of upflowing solids to exit the riser. The type of exit had a large influence on the solids distribution in the upper part of the riser. Brereton (1987) introduced the concept of a reflection coefficient, R_f (a measure of the degree of reflection due to the exit bend, evaluated at the top of the riser just below the exit), to interpret his results. A reflection coefficient was also used by Senior (1992) to interpret his results. Senior defined R_f as the ratio of downwards solids flow to upwards solid flow in the riser. He demonstrated that abrupt or small-area exits give high values of R_f, while smooth or large-area exits give low values.

Based on extensive experiments, Brereton and Grace (1994) concluded that the exit geometry can influence pressure and density profiles along a considerable length of the riser. In an earlier article, however, Grace (1990) reported the exit effect to extend along the whole length of the riser. Brereton and Grace (1994) used a reflection coefficient to help explain the observed profiles, although as a qualitative measure only.

Mickal et al. (2001) also used a reflection coefficient to demonstrate the effect of exit geometry. They performed experiments in a circular riser equipped with a blind-T exit with

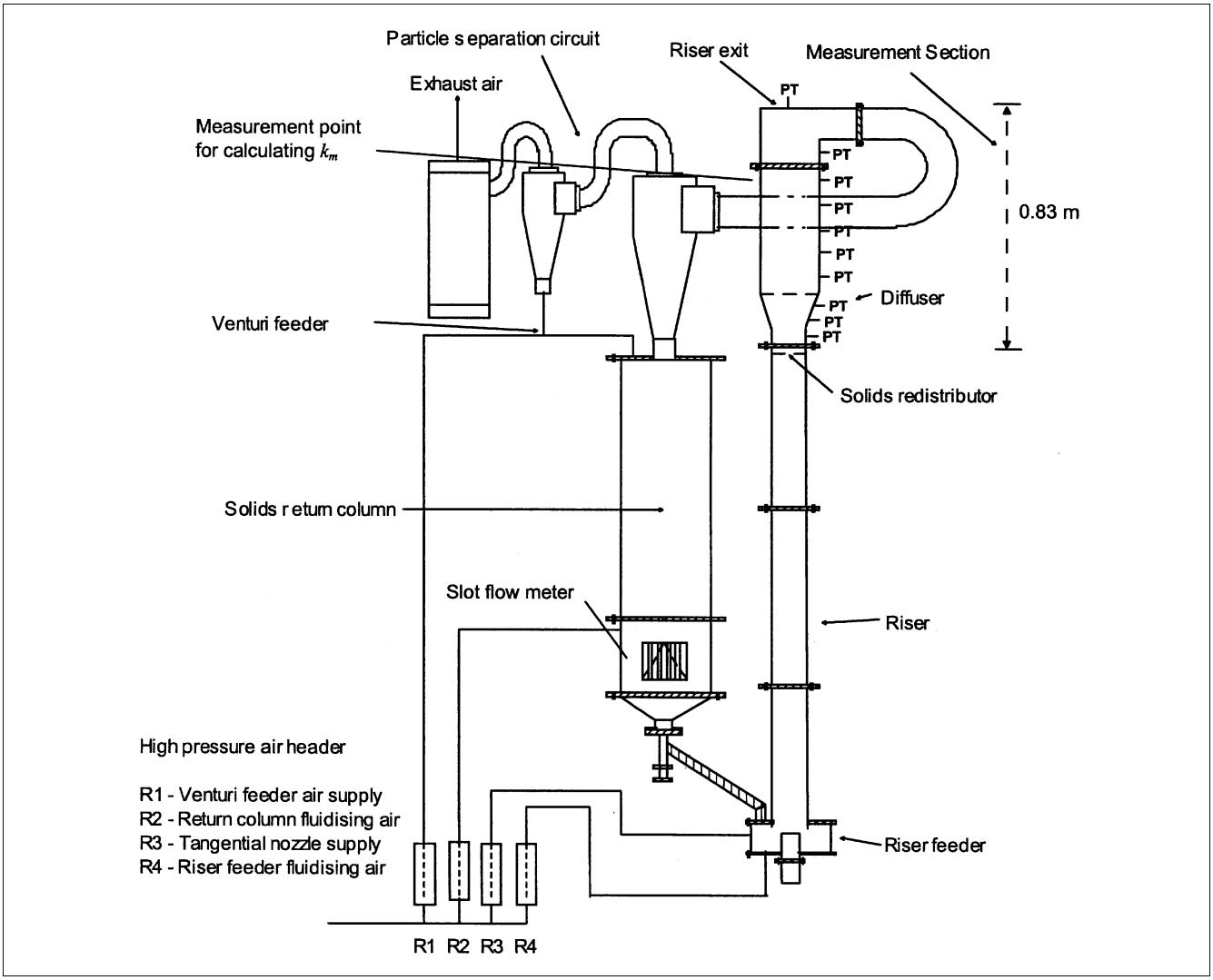

Figure 1. Experimental unit.

Measurement section is indicated.

three different capped extensions at the top of the bend. The particles used were classified as Geldart C solids (that is, small and highly cohesive). The results of their study indicated that the exit geometry significantly affects the internal solids back mixing in a riser operating with these types of particles.

Jin et al. (1988) and Jin et al. (1997) concluded from their studies that riser exit structures can significantly affect flow conditions in the lower regions of a riser as well as in the direct vicinity of the exit. Their conclusions in this regard are in agreement with those of Brereton and Grace (1994).

Johnsson et al. (1999) performed experiments on a cold 1/9 scale model of the Chalmers University 12-MW CFB boiler, using three different versions of a square cross-section abrupt exit (basic abrupt, capped abrupt, and extended capped abrupt) and a number of different internal baffles within the exit zone. The authors determined that the influence on the exit pressure drop from the capped extensions was minimal, and in many of their experiments no solids were observed in the capped extension. This is in contrast with the results reported by Zheng and Zhang (1994), who demonstrated the length of the capped extension at the exit affected the riser exit pressure drop significantly.

The most comprehensive study to date is that of Pugsley et al. (1997). They measured axial pressure profiles in risers of different diameters and heights, containing sand or FCC particles (Geldart D and A solids, respectively). The influence of the exit varied significantly for the different conditions studied, and ranged from the whole length of the riser to the upper region only. The mechanism put forward by the authors to explain their results suggested that if the riser diameter and particle terminal velocity were large enough, the exit effect can extend all the way to the base of the riser. This will be discussed in greater detail later.

van der Meer et al. (2000) conducted experiments with seven different exits in a square cross-section riser. They presented their results as a reflux ratio, similar to the reflection coefficient presented by Brereton (1987), Senior (1992), and Brereton and Grace (1994), but based upon extensive local radial solids flux measurements made in the riser, just below the exit. van der Meer et al. defined the reflux ratio as

$$k_m = \frac{\text{Solids downflow in the riser at the entry to the exit}}{\text{External-solids circulation rate}}.$$

They found that this reflux ratio varied by a factor of 25, according to the exit design.

The authors also briefly discussed the concept of a Froude number introduced by van der Meer (1997) to help explain the motion of solids in a riser exit. Owing to their high density, solids in the core region of a riser exit may slip either to the outside or inside of the exit, depending upon the relative magnitudes of their centrifugal acceleration and acceleration due to gravity. The ratio of centrifugal acceleration to gravity can be represented by a riser-exit Froude number defined as

$$Fr_R = \frac{u_{st}^2}{gR} \tag{1}$$

Table 2. Experimental Parameters

Parameter	Oper. Cond. for Slough CFBC	Scaled Cond. for Similarity with Slough CFBC	Range for Exp.
U_g (Superficial gas vel., m/s)	7	1.3	1.3
G_g (Solids circ. flux, kg/m^2·s)	18	2.2	1.5–5.5
d_p (Mean particle dia., μm)	200	67	48
ρ_p (Particle density, kg/m^3)	2,600	1,700*	1,700
ρ_g (Gas density, kg/m^3)	0.3	1.2*	1.2
U_t (Particle terminal vel., m/s)	0.98	0.18**	0.11
D (Hydraulic dia., m)	4.0	0.15*	0.15
H (Short riser hgt., m)	20	0.83	0.83
μ (Gas vis., Pa·s)	4.5×10^{-5}	1.8×10^{-5}	1.8×10^{-5}
H/D	5.6	5.5	5.5

*Chosen independently.
**Dependent parameter.

In Eq. 1, u_{st} is the mean solids velocity at the entry to the riser exit, and R is the average radius of curvature of the exit bend.

Experimental Studies

A series of experiments were performed to investigate the influence of exit geometry on the riser axial solids concentration profile. Concentration profiles were calculated from time-averaged riser pressure-profile measurements made in a laboratory-scale CFB unit. The section of the riser used for measurement was geometrically similar to a Battelle industrial CFB combustor operating at Slough Industrial Estates in the UK. Scaling was performed using three groups for dimensional consistency (van der Meer, 1997). The basic experimental unit is illustrated in Figure 1. The measurement section was restricted to the upper 0.83 m of the riser, giving an H/D ratio of 5.5. It had a square cross section and contained a diffuser. The bed solids were a silica alumina FCC described by van der Meer (1997) and Harris (1993); Table 2 gives mean particle size and density. The lower portion of the riser was separated from the measurement section by a perforated-plate solids distributor with 2-mm holes to give 47% total free area. The purpose of this distributor was to make a small section of an academic riser (with the appropriate height-to-diameter ratio for a CFB combustor) behave with the typical hydrodynamics of the whole riser of the industrial unit. Preliminary pressure-profile experiments were conducted to ensure that similarity was achieved. These profiles indicated a dense bed at the base of the riser extending to a less dense region above this, consistent with pressure-profile measurements in larger-scale CFB combustors [see, for example, Johnsson et al. (1999)]. The range of operating conditions chosen for experimentation and values of typical experimental parameters for the industrial combustor are given in Table 2. Values of solids flux and superficial gas velocity were selected to fit with the scaling calculations for the industrial riser (Table 2, column 2). Solids flux was measured using a slot flowmeter (Harris, 1993), and the superficial gas velocity was measured using an annubar. Full details of the experi-

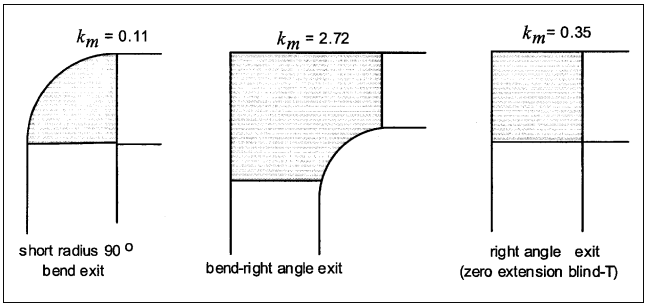

Figure 2. Exit bends and typical reflux ratios calculated at the entrance to the exit.

mental setup are reported in van der Meer (1997) and van der Meer et al. (2000).

The exit bends used in this study were chosen based upon their representative reflux ratios (k_m), as reported by van der Meer (1997). The three exits used are illustrated in Figure 2. The first, a smooth internally baffled, right-angle bend had a typical reflux ratio of 0.11. This type of bend is often referred to as a "smooth exit." The second exit, a large-radius bend/right-angle exit had a typical reflux ratio of 2.72. This exit was designed to give the maximum possible refluxing effect. The third exit was a right-angle bend of the same radius of curvature as the internally baffled exit, with a typical reflux ratio of 0.35. The first two exits illustrate behavior at the extremes of the influence of the exit geometry, and the third is similar to those most commonly used in industrial CFB combustors. All the reflux ratios were calculated from solids flux measurements made at the entrance to the riser exit (see Figure 1) using a pitot-tube-type suction probe. The net local solids mass flux was assumed to be equal to the difference between the fluxes measured by the probe facing in the upwards and downwards directions. Full details are presented in van der Meer (1997).

To calculate the cross-sectional averaged solids volume fraction, $(1-\epsilon)$, from the pressure profile, the following relation was used

$$\frac{dP}{dz} = \rho_p \cdot g \cdot (1-\epsilon) = \rho_p \cdot g \cdot \bar{\epsilon}_s \qquad (2)$$

Here P is the pressure, measured by wall tappings, ϵ is the voidage fraction, ρ_p is the particle density, $\bar{\epsilon}_s$ is the cross-sectional averaged solids volume fraction, and g is the acceleration due to gravity.

Equation 2 assumes that suspended solids constitute the sole contribution to the pressure drop, and is valid only in regions where friction and acceleration effects are negligible. The use of time-averaged pressure profiles to infer local solids concentrations is widespread, and the reliability of Eq. 2 has been demonstrated for a riser operating without secondary air injection (Arena et al., 1986). In our experiments, using the pressure tappings (PT) in Figure 1, the reported solids concentration profiles were corrected for an accumulation of solids in the pressure lines during each experiment, by measuring the residual pressure drop due to these solids at the completion of each run with the riser empty. Several repeats were performed at each set of conditions to ensure reproducibility in the measured profiles.

Results

Comparative results giving $\bar{\epsilon}_s$ as a function of distance, h, above the base of the riser, for the three different riser exits, are presented in Figures 3, 4, and 5. In each figure, the influence of the exit geometry on the profile is clear and for each set of experimental conditions the solids concentration profile shifts appreciably toward higher values, in line with an increase in the refluxing effect of the exit. This trend is consist-ent with results reported by other authors [Zheng and Zhang (1994), Brereton and Grace (1994), and Pugsley et al. (1997)] in circular cross-section risers, and van der Meer et al. (2000) in square cross-section risers. The results presented are also in agreement with the study of Martin et al. (1992a), the only one performed in an industrially sized CFB unit (D = 0.94 m, H = 26 m).

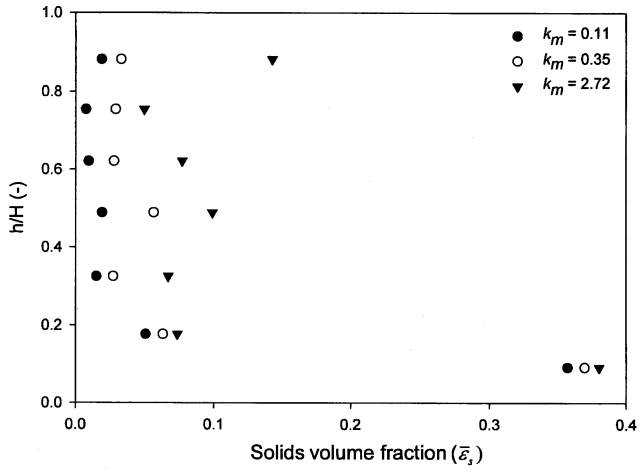

Figure 3. Axial solids concentration profile for FCC particles.

G_s = 1.5 kg/m^{2}s; U_g = 1.3 m/s; D = 0.14 m; riser height = 0.83 m.

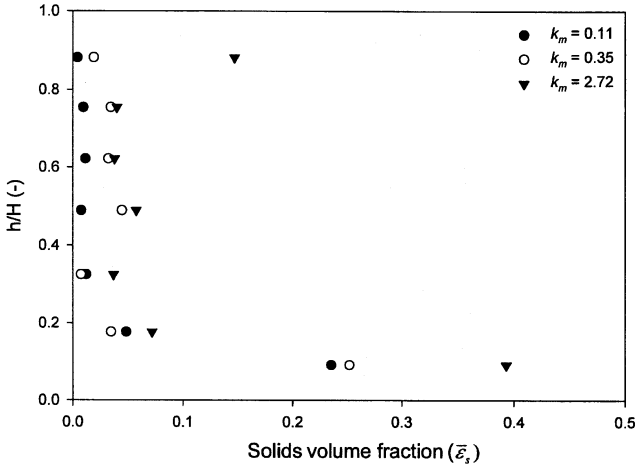

Figure 4. Axial solids concentration profiles for FCC particles.

G_s = 2.2 kg/m^{2}s; U_g = 1.3 m/s; D = 0.14 m; riser height = 0.83 m.

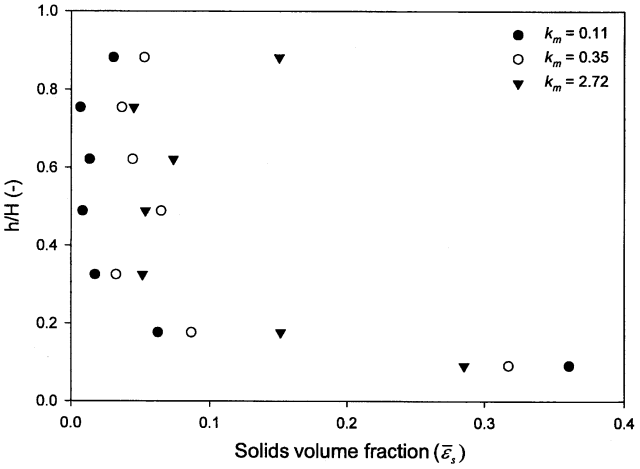

Figure 5. Axial solids concentration profiles for FCC particles.

$G_s = 5.5$ kg/m^{2}s; $U_g = 1.3$ m/s; $D = 0.14$ m; riser height = 0.83 m.

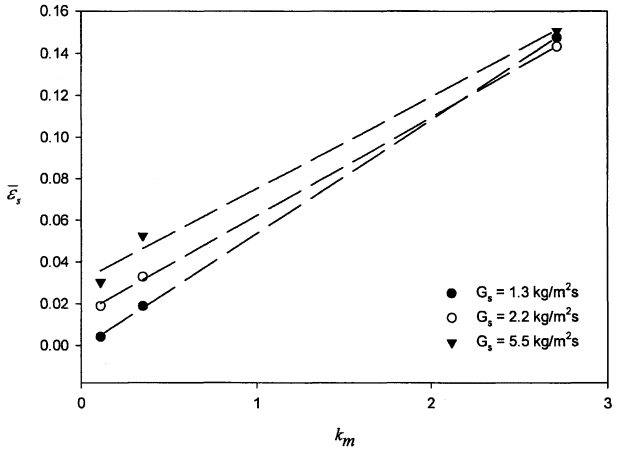

Figure 6. Increase in cross-sectional averaged solids concentration ($\bar{\varepsilon}_s$) at the top of the riser ($h/H = 0.9$) vs. reflux ratio (k_m).

The profiles (Figures 3–5) for the internally baffled exit (typical $k_m = 0.11$) indicate a dense bed at the riser base and then a region of relatively constant $\bar{\epsilon}_s$ along the remainder of the riser. For this exit (typical $k_m = 0.11$), a slight increase in the local solids concentration at the top ($h/H = 0.9$) was observed at the highest superficial solids flux, G_s (see Figure 5 as compared to Figures 3 and 4). Visual observation of flow at the exit confirms the majority of solids exit the riser in a single pass. Very little refluxing was observed.

Profiles for the abrupt right-angle exit (typical $k_m = 0.35$) similarly indicate the presence of a dense bed at the riser base. All profiles for this exit exhibit an increase in solids concentration at the same height when compared with the minimum refluxing bend (typical $k_m = 0.11$). Some rebounding of solids from the roof of the exit, back down into the riser was observed, although this does not appear to increase the local solids concentration observed at the exit. Solids were also observed to fall back into the riser along the inside of the exit bend.

For the maximum refluxing exit (typical $k_m = 2.72$), a significant increase in solids concentration at the top ($h/H = 0.9$) is observed in addition to the increased solids concentration at each axial location, when compared with the minimum refluxing exit (typical $k_m = 0.11$). The resulting profile matches well with that reported by Lim et al. (1995) as a C-shaped profile caused by significant refluxing of solids at the exit. Visual observation supports this conclusion. A large quantity of solids were observed to slide along the inside of the bend back into the riser. Some rebounding from the abrupt roof of the exit was also observed.

For all the experimental profiles presented in Figures 3, 4 and 5, a buildup of solids was observed downstream of the exit bend in the horizontal connecting section between the exit and the primary cyclone. During operation, solids were observed to fall down the face of the pile, returning to the riser along the inside of the exit bend.

The results presented in Figures 3, 4 and 5 confirm results from earlier studies in circular "small" scale risers [Brereton and Grace (1994), Jin et al. (1988), Zheng and Zhang (1994), Mickal (2001), and Pugsley et al. (1997)]. These authors found that the exit geometry can have a significnat influence on the hydrodynamics of a CFB riser. This is encouraging given the results presented here are for a square cross-section riser with a height-to-diameter ratio of 5.5 (consistent with the industrial CFB combustor in Table 1). Typical academic risers can have height-to-diameter ratios approaching 100. The apparently linear correlation between reflux ratio (corresponding to the refluxing effect of the exit) and the increase in cross-sectional averaged solids concentration just below the exit is illustrated in Figure 6.

In analyzing the data in Figures 3, 4, and 5, it is important to consider the potential uncertainties linked with the pressure-profile measurements in fast fluidized beds. The inherent nature of two-phase riser flow has a random component, and fluctuations in local pressures do occur. However, the observed increase in local solids concentration between the smooth exit and the abrupt exits at the conditions studied cannot be attributed to random pressure fluctuations only. In the vicinity of the exit, the observed increase in apparent local solids concentration is of an order of magnitude greater than that due to random pressure fluctuations alone. The resutls presented in Figures 3, 4, and 5 are typical of profiles gathered from many experiments at the conditions studied and are, therefore, reproducible. Concerns about the inherent nature of riser flow and the interpretation of pressure-profile data were also discussed in detail by Pugsley et al. (1997) and support our conclusions.

Discussion

Mechanism of solids refluxing at the riser exit

Numerous physical mechanisms have been proposed to help explain the refluxing of solids observed in the vicinity of riser exits. All propose essentially the same type of flow in the exit region, although there are slight variations depending upon the exact geometry, that is, whether the exit is perceived to be abrupt or smooth.

Jin et al. (1988) and Bai et al. (1992) proposed three regions of solids behavior in the vicinity of an abrupt exit with capped extension as follows:

(1) A region where solids strike the exit cap and accumulate. The flow direction is altered and the motion of gas and solids is accompanied by vigorous back mixing. Some solids and the gas pass through the exit to the solids separation circuit.

(2) A region of solids momentum exchange below this, where the downflowing solids, emanating from the exit cap interact with the upflowing solids in the riser.

(3) A region further down of typical fast fluidized-bed conditions, outside the influence of the exit.

Jin et al. (1988) developed a linear correlation between the length of the momentum exchange region (Z) and a gas Reynolds number. This mechanism proposed by Jin et al. (1988) and Bai et al. (1992) suggests the influence of the exit cannot extend to the base of the riser.

Brereton (1987), Senior (1992), and Brereton and Grace (1994) suggested that inertial separation due to rebounding of solids at the exit affects pressure-profile measurements. Solids separate from the gas stream (to the outside of the bend) as it accelerates and is made to turn abruptly in a short space. The authors defined the reflection coefficient, R_f (see earlier and Eq. 9 below), which expressed the fraction of solids reflected back down the walls of the column in terms of the upwards and downwards particle velocities in the respective core and annulus regions of the riser. The mechanisms proposed by Brereton, Senior, and Grace do not consider solids returning to the riser along the inside of the exit bend, although the reflection coefficient does take quantitative account of these solids.

Pugsley et al. (1997) proposed a general shearing action of the upward-flowing gas phase on the downward-flowing annular solids, similar in concept to the region of momentum exchange defined by Jin et al. (1988) and Bai et al. (1992). It was postulated that solids possessing a low terminal velocity are likely to travel some dependent distance below the exit before being entrained by the upward-flowing gas, whereas solids with larger terminal velocities may possess enough momentum to reflux all the way to the base of the riser. Pugsley et al. (1997) also suggested that the formation of clusters might enable groups of particles to interact with the upward-flowing gas stream, causing them to become reentrained. These hypotheses only account for the behavior of solids that have refluxed from the exit and do not explain the motion of solids in the exit itself.

All the mechanisms described are based primarily on physically observed flow patterns in the vicinity of the riser exit. They are able to account qualitatively for the observed pressure profiles measured here, as well as those made in earlier studies, but do not account for the full mechanism of solids flow within the exit.

In addition to the physical models described earlier, van der Meer (1997) presented the concept of an exit Froude number (Eq. 1) to help explain the motion of solids in a riser exit (as opposed to upstream of the exit). van der Meer (1997) postulated that solids would follow a curved path of the mean radius R at the exit, and, hence, the centrifugal acceleration u_{st}^2/R could be balanced against the average component of the acceleration due to gravity, g cos(45°), acting toward the center of the bend (Figure 7). Large values of Fr_R would indicate the movement of solids to the outside of the bend, while small Froude numbers would indicate the movement of the solids to the inside of the bend. van der Meer showed some evidence that recycle is minimal when $Fr_R = 1\sqrt{2}$, that is, when the mean gravitational and centrifugal acceleration are balanced. He also gives clear evidence that with low exit Froude numbers recycle is high, as in the case of a large radius bend.

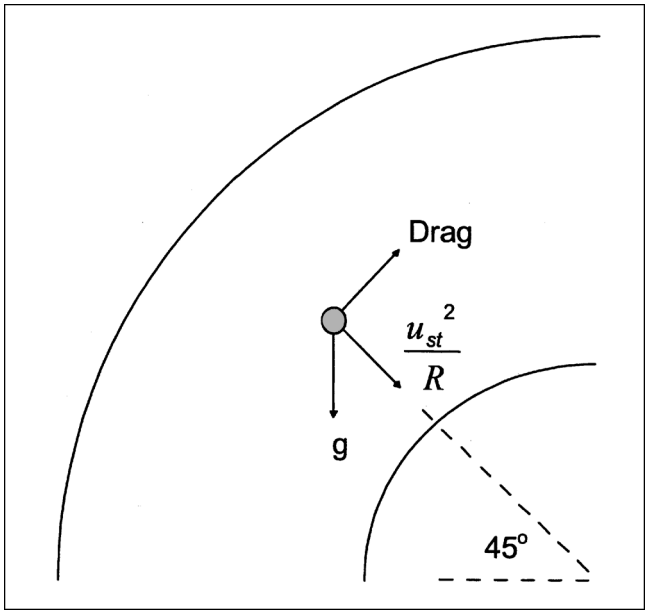

Figure 7. Forces acting on a single particle traveling through a curved bend.

Figure 8 shows the behavior of gas and solids in the riser exit consistent with the Froude number concept. This mechanism places as much emphasis on the return flow of solids along the inside of the exit bend (from the solids buildup to the riser annulus) as it does to solids rebounding from the

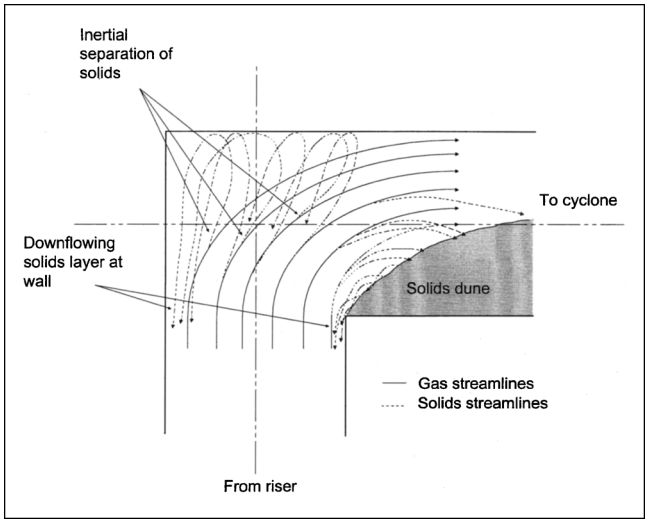

Figure 8. Physical mechanism of solids refluxing within the riser exit.

roof (or capped extension) and moving to the outside of the exit bend. Upstream of the exit, the mechanisms presented by other investigators are likely to be important in predicting local solids concentrations: these mechanisms include the interaction of clusters with the upflowing gas stream and the exchange of momentum between upflowing and downflowing solids.

Measures of the exit effect

To test the validity of a riser exit Froude number for describing the relative refluxing effects of different riser exits, three measures of the exit effect are used. These are as follows:

(1) A comparative dimensionless length of influence (Ω) of abrupt and smooth riser exits; Ω compares differences in pressure profiles from identical risers equipped with different exits, operating at the same conditions and is defined as

$$\Omega = \frac{\text{Length of influence}}{\text{Riser height}}$$

where the length of influence is the distance along the riser from the top, where the pressure profiles from smooth and abrupt exits coincide.

(2) The exit reflection coefficient (R_f) defined by Senior (1992) as the ratio of (downward solids flow in riser)/(upward solids flow in riser) just below the riser exit.

(3) The comparative increase (between abrupt and smooth riser exits) in cross-sectional averaged solids concentration at the exit.

The Froude number was calculated according to Eq. 1. Each value of u_{st} was calculated from the measured pressure gradient, dP/dZ, immediately below the exit bend. From this dP/dZ, the solids volume fraction, $\bar{\epsilon}_s$, was calculated from Eq. 2, giving u_{st} from the continuity relation

$$G_s = \rho_p u_{st} \bar{\epsilon}_s \tag{3}$$

Here G_s is the mean solids flux calculated from the measured external solids circulation rate from the slot flowmeter in Figure 1.

Dimensionless length of influence of a riser exit

The influence of the exit, expressed as a dimensionless length of influence, Ω (similar to the length of momentum exchange (Z) reported by Jin et al. 1988), was determined. This length of influence is calculated by comparing axial pressure profiles measured at the same operating conditions in identical risers equipped with different exits and is a measure of how far the exit effect extends down the riser. It is made nondimensional with riser height.

Our results, as well as those from the studies of Brereton (1987), Pugsley et al. (1997), Jin et al. (1988), and Zheng and Zhang (1994) were used in the analysis.

The comparative length of influence was plotted against a version of the Froude number different from that in Eq. 1. Because Ω compares the influence of exit geometry between abrupt and smooth exits, the Froude number was calculated using the change in average particle velocity ($\Delta \bar{u}_{p,\text{exit}}$) due to the influence of the exit. For either abrupt or smooth exits, the average solids velocity at the entrance to the exit is given by Eq. 3, so the change in solids velocity, from one to the other, is

$$\Delta \bar{u}_{p,\text{exit}} = f \frac{G_s}{\rho_p} \left(\frac{1}{(\bar{\epsilon}_{s,\text{abrupt}})} - \frac{1}{(\bar{\epsilon}_{s,\text{smooth}})} \right) \tag{4}$$

The values of $\bar{\epsilon}_{s,\text{abrupt}}$ and $\bar{\epsilon}_{s,\text{smooth}}$ were obtained from the measured pressure gradient immediately below each exit bend, using Eq. 2 with the measured external solids circulation rate. The comparative exit Froude number is then defined as

$$Fr_C = \frac{\Delta \bar{u}^2_{p,\text{exit}}}{gR} \tag{5}$$

To use the published data sets, an estimate of the radius of curvature, R, of the exit bend was required. This radius was calculated by assuming the exits used in the reported studies had a geometric similarity with riser exits of the known radius of curvature. The estimated R was then calculated by scaling according to the riser diameter. Where the inlet and outlet of the exit were of a different radii, R was defined by

$$R = \sqrt{R^2_{\text{in}} + R^2_{\text{out}}} \tag{6}$$

where R_{in} and R_{out} are the respective center-line radii of curvature at the inlet and outlet of the exit bend.

The results of the analysis are presented in Figure 9. At low values of Fr_C the length of influence of the exit geometry (that is, the exit effect) is high. As Fr_C increases, Ω decreases to a minimum value of approximately 4. This is consistent with the findings of van der Meer (1997) and might be explained as follows.

For a smooth exit, one would expect the mean solids velocity at the exit to be large and the corresponding mean exit solids concentration to be small, because of the low refluxing effect (that is, most solids exit the riser in a single pass and little refluxing is observed). For an abrupt exit the opposite trends would be expected (that is, a higher mean exit solids concentration giving a lower mean solids velocity), corresponding to a high refluxing effect. One would expect that

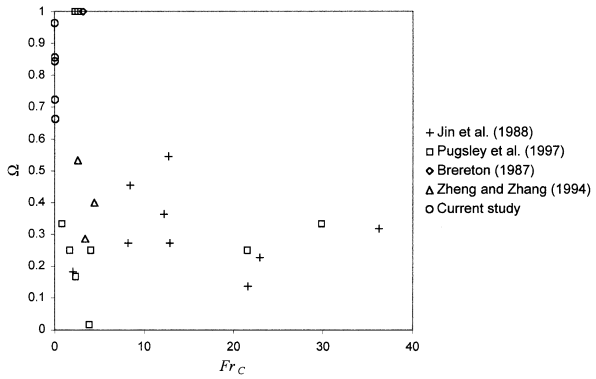

Figure 9. Influence of riser exit geometry (Ω vs. Fr_C), using the comparative exit Froude number.

for more abrupt exits, there would be larger absolute values of

$$\left(1/\left(\bar{\epsilon}_{s,\text{abrupt}}\right) - 1/\left(\bar{\epsilon}_{s,\text{smooth}}\right)\right)$$

and consequently smaller values of $\Delta\bar{u}_{p,\text{exit}}$ from Eq. 4. Hence, low comparative exit Froude numbers (defined in Eq. 5) are expected for highly refluxing exits. For relatively smooth exits (that is those with lower solids refluxing capability), the opposite trend would be expected, leading to higher values of the comparative exit Froude number.

There is some uncertainty in the results presented in Figure 9 because of the need to estimate a value for the radius of curvature of the exit bend (information not explicitly reported in any of the studies used in the analysis) and the uncertainty in estimating the value of Ω from experimental pressure profiles. However, the basic trend just outlined is apparent across the range of data presented. When the influence of the exit is great (that is, high values of Ω), the corresponding Fr_C is low. Values of Fr_C then taper off at lower values of Ω. It is possible that a local minimum of Fr_C may exist, as suggested by van der Meer (1997); however, the lack of suitable data means it is not possible to establish the existence of a minimum in Fr_C. Uncertainties are also introduced by the fact that not all the abrupt exits studied are of exactly the same type and will, therefore, have different effects upon solids refluxing.

Correlation to predict Ω

Attempts were made to extend the analysis by correlating Ω with particle properties and operating conditions (G_s, U_g, D), as is clear from the results reported here and in previous studies, that the length of influence of the riser exit is influenced by the riser and riser exit geometry, experimental conditions, and particle properties. Thus

$$\text{Length of influence} = f\left(d_p, \rho_p, U_g, U_t, G_s, \rho_g, \mu_g, D, H, R, g\right) \tag{7}$$

Analysis of Eq. 7 yielded the following dimensionless groups

$$\Pi_1 = \frac{G_s}{\rho_p\left(U_g - U_t\right)} \quad \Pi_2 = \frac{\left(U_g - U_t\right)^2}{gD}$$

$$\Pi_3 = \frac{\rho_g\left(\rho_p - \rho_g\right)\cdot g \cdot d_p^3}{\mu^2} \quad \Pi_4 = \frac{d_p}{D} \quad \Pi_5 = \frac{\rho_p U_g D}{\mu_g}$$

$$\Pi_6 = \frac{R}{D} \quad \Pi_7 = \frac{H}{D} \quad \Pi_8 = \frac{\text{LOI}}{H}$$

where LOI is the length of influence of an abrupt exit geometry compared with a smooth one (that is, $\Pi_8 = \Omega$). The LOI was determined by comparing pressure profiles from risers operating at the same conditions equipped with abrupt and smooth exits, and was the axial distance from the riser exit where the pressure profiles coincided, as described earlier. A plot of Π_8 vs. Π_1 at constant values of Π_2 through Π_7 is illustrated in Figure 10 for the results presented in Figures 3, 4, and 5 and the experimental data of Jin et al. (1988) and Zheng and Zhang (1994). A correlation of the form

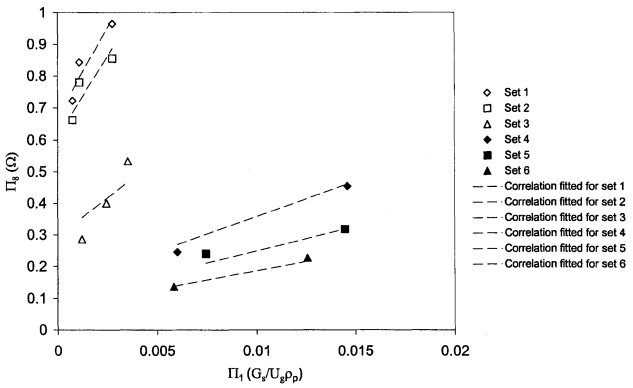

Figure 10. Correlation of the exit effect, for six sets of data from Figures 3, 4, 5 and the results of Jin et al. (1988) and Zheng and Zhang (1994).

Each at constant values of Π_2 through Π_7; for each set of data points, the correlation fit (Eq. 9) is the line closest to those data points.

$$\Pi_8 = \left(A + B\cdot\Pi_1\right)\cdot\Pi_2^a\cdot\Pi_3^b\cdot\Pi_4^c\cdot\Pi_5^d\cdot\Pi_6^e\cdot\Pi_7^f \tag{8}$$

was developed from the combined data set by minimizing the sum of the squares of the errors. The final form of the correlation is

$$\Omega = \left(0.046 + 8.37\left(\frac{G_s}{\left(U_g - U_t\right)\rho_p}\right)\right)\left(\frac{\left(U_g - U_t\right)^2}{gD}\right)^{-0.52} \times\left(\frac{\rho_g\left(\rho_p - \rho_g\right)\cdot g\cdot d_p^3}{\mu^2}\right)^{0.22}\left(\frac{d_p}{D}\right)^{-0.08}\left(\frac{\rho_p U_g D}{\mu_g}\right)^{0.23} \times\left(\frac{R}{D}\right)^{0.05}\left(\frac{H}{D}\right)^{-0.28} \tag{9}$$

with an average percentage error of 4.5% in relation to the data used. The data were collected at the conditions shown in Table 3, giving the range of values where Eq. 9 is applicable.

Figure 11 shows a comparison between the correlation (Eq. 9) and the full data set, which includes all available data, not merely the values used to generate the correlation. The comparative length of influence (Ω) is successfully predicted for all cases except results reported by Pugsley et al. (1997). These experiments were performed at conditions outside the range listed in Table 3 (that is, with Geldart D solids), which contributes greatly to the deviation. The rms deviation between the prediction and all available data, including that of Pugsley et al. (1997), is $\pm 15\%$.

Exit reflection coefficient

A further measure of the exit effect in CFB risers is the exit reflection coefficient, R_f, developed by the UBC research group. The Froude number of van der Meer (1997)

Table 3. Conditions to Generate Eq. 9

Parameter	Values	Groups	Values
G_s	1.5–180 kg/m^2·s	Π_1	0.00057–0.016
U_g	1.3–6.24 m/s	Π_2	1.2–46.0
D	0.10–0.14 m	Π_3	7–8,447
H	0.83–11.0 m	Π_4	0.00034–0.0054
d_p	48–550 μm	Π_5	12,133–85,333
ρ_p	711–1,700 kg/m^3	Π_6	0.5–2
ρ_g	1.2 kg/m^3	Π_7	5.9–78.6
R	0.07–0.25 m	Π_8	0.017–1

Source: Data from Figures 3, 4, and 5, and from Jin et al. (1988) and Zheng and Zhang (1994).

defined in Eq. 1 was plotted against the exit reflection coefficient (R_f) defined by Senior (1992)

$$R_f = \frac{\left(\frac{G_s}{u_{p,\mathrm{up}}} - \rho_b\right)}{\left(\frac{G_s}{u_{p,\mathrm{dn}}} - \rho_b\right)} = \frac{k_m}{1+k_m} \tag{10}$$

In Eq. 10, ρ_b is the suspension density averaged over the riser cross section and $u_{p,\mathrm{up}}$ and $u_{p,\mathrm{dn}}$ are the upward and downward particle velocities, respectively, in the vicinity of the exit, each averaged over the riser cross section. The reflection coefficient is predominantly used qualitatively; however, it is also possible to use R_f to quantify the exit effect (Senior, 1992). For R_f to be a useful measure, the respective upwards and downwards solids velocities need either to be known (from experiment) or estimated. If the riser is considered to consist of a core–annulus structure, then the upwards particle velocity, $u_{p,\mathrm{up}}$ can be estimated as

$$u_{p,\mathrm{up}} = U_g\left(\frac{A_{cs,\mathrm{riser}}}{A_{cs,\mathrm{core}}}\right) - U_t \tag{11}$$

where $A_{cs,\mathrm{riser}}$ and $A_{cs,\mathrm{core}}$ are the respective cross-sectional areas of the riser and core. The cross-sectional area of the core can be estimated using the correlation of Bi et al. (1996), which expresses the relative thickness (δ_f) of the downflowing annular film as a function of the riser cross-sectional solids concentration ($\bar{\epsilon}_s$)

$$\frac{\delta_f}{D} = 0.5^*\left[1 - \sqrt{1.34 - 1.30(\bar{\epsilon}_s)^{0.2} + (\bar{\epsilon}_s)^{1.4}}\right] \tag{12}$$

where $0.0015 \le \bar{\epsilon}_s \le 0.2$.

The data collated by Bi et al. (1996) were from a large number of experimental studies in square and circular cross-section risers ranging from 0.05 m to 8 m in diameter. Measured values of δ_f/D ranged from 0.011 to 0.13. We can then calculate A_{cs} using the film thickness (δ_f) from

$$D = D_c + 2\delta_f \tag{13}$$

and

$$A_{cs} = \frac{\pi D_c^2}{4} \tag{14}$$

Senior (1992) assumed a constant value for the annular velocity of -1.1 m/s. Based on the range of reported values for cluster velocity documented by Glicksman (1997) and the results of more recent research (Harris et al., 2002), this is a valid estimate. In the analysis reported here, $u_{p,\mathrm{down}}$ was varied over a range of values (-0.5 m/s to -1.5 m/s) to gauge the effect of uncertainty as to $u_{p,\mathrm{down}}$.

The experimental data measured in this study as well as the results reported by Senior (1992), Brereton (1987), Zheng and Zhang (1994), Jin et al. (1988), van der Meer (1997), and Pugsley et al. (1997) were used to obtain estimates of the values of R_f. Values for the cross-sectional average suspension density (ρ_b) at the riser exit were calculated from Eq. 2 using the pressure-profile data reported in the individual studies.

The results are presented in Figures 12 and 13. Figure 12a illustrates the relationship between Fr_R and R_f for smooth exits, and Figure 12b illustrates the relationship for abrupt exits. For the data in these plots, it was assumed that $u_{p,\mathrm{down}} = -1.1$ m/s, following Senior (1992). The clear relationship between Fr_R and R_f is surprising given the uncertainties in the reported data, the difficulty in estimating R from the variety of exit geometries, and the need to estimate values of the respective upwards and downwards particle velocities. The results in Figure 12 provide further evidence that flow in the vicinity of a riser exit can be characterized in terms of a Froude number. The data in Figures 12a and 12b were fitted to a function of the form

$$R_f = 1 + \frac{aFr_R^b}{c^b + Fr_R^b}$$

and the resulting correlation is

$$R_f = 1 + \frac{-1.05Fr_R^{0.51}}{0.30^{0.51} + Fr_R^{0.51}} \tag{15}$$

Figure 13 illustrates the whole data set and the model prediction from Eq. 15. The standard sum-of-squares error is 3.8%, and the correlation coefficient (R^2) is 0.98. Figure 13 and

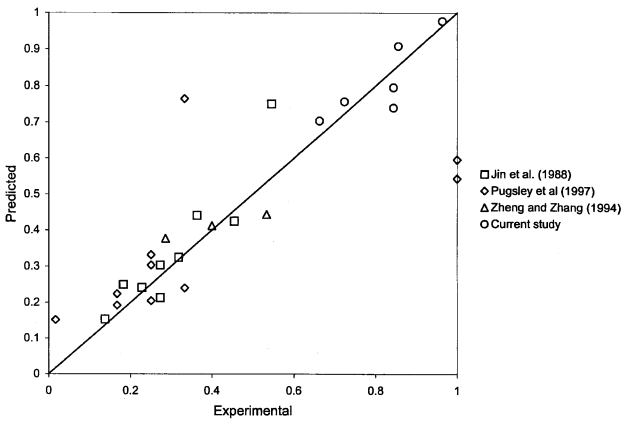

Figure 11. Predicted vs. actual values of Ω using Eq. 9.

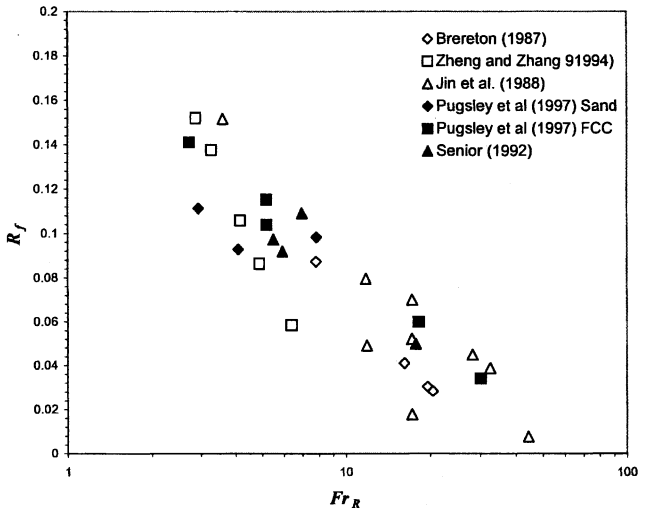

a) smooth exits

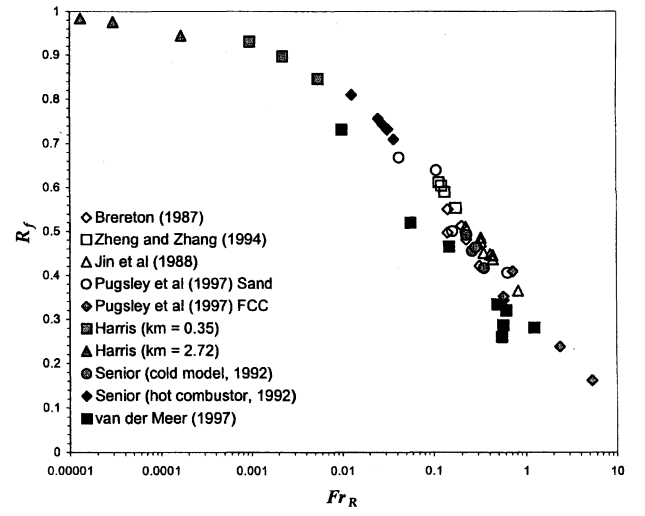

b) abrupt exits

Figure 12. Calculated R_f vs. Fr_R: (a) smooth exits; (b) abrupt exits.

Eq. 15 are useful scale-up tools that can be used by CFB designers to predict the degree of influence (that is the quantity of refluxed solids) likely to result from a specific exit configuration (defined by an exit Froude).

The exit reflection coefficient, R_f, is a useful measure of the exit effect and effectively quantifies the influence of different exit configurations on the riser pressure profile. The values plotted in Figure 13 are based on the prediction of δ_f from Bi et al.'s (1996) correlation and on the assumption of constant $u_{p,\text{down}}$. van der Meer's (1997) values of the reflux ratio are directly based on solids flux measurements at the entrance to the exit and do not have the element of uncertainty in the values plotted in Figure 13.

Comparative increase in solids concentration at the exit

Jin et al. (1988) developed a linear correlation between the length of the momentum exchange zone, Z (similar to Ω),

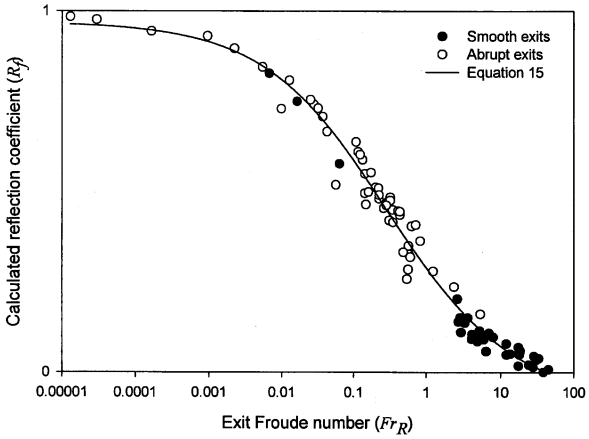

Figure 13. Analysis of riser exits (R_f vs. Fr_R) and model prediction from Eq. 15.

and a gas-phase Reynolds number. They also postulated a linear correlation between G_s and the increase in apparent solids concentration at the exit. The full set of experimental results analyzed in this article were treated in the same manner. There was no clear trend in plots of Re vs. the maximum increase in solids concentration at the exit, $\Delta\bar{\epsilon}_{s,\text{exit}}$; however, a plot of the gas–solid flow-rate ratio (Π_1) vs. $\Delta\bar{\epsilon}_{s,\text{exit}}$, defined below, gave some indication of a correlation between the two for each set of reported results (see Figure 14). Here $\Delta\bar{\epsilon}_{s,\text{exit}}$ is defined as

$$\Delta\bar{\epsilon}_{s,\text{exit}} = \bar{\epsilon}_{s,\text{exit(abrupt)}} - \bar{\epsilon}_{s,\text{exit(smooth)}} \tag{16}$$

that is, the comparative maximum increase in cross-sectional averaged solids concentration at the riser exit between abrupt and smooth exits. A relationship between G_s and the maximum observed pressure drop at the riser exit ($dP_{\text{exit}} - dP_{\min}$) was also observed for abrupt exits (Figure 15). In Figure 15, dP_{exit} is the measured pressure drop at the riser exit and $dP_{\min}$

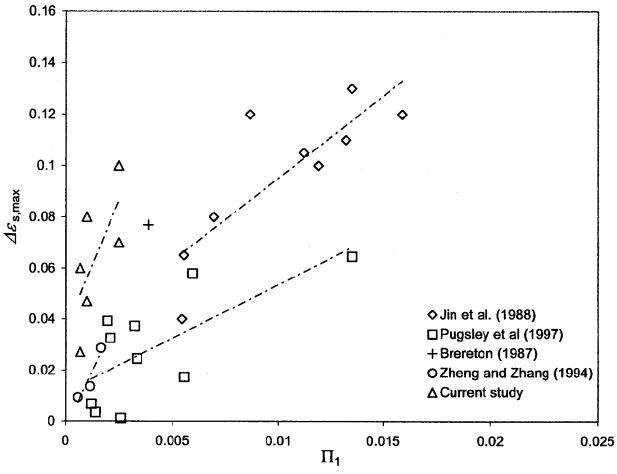

Figure 14. Correlation between maximum increment of solids density at the riser exit ($\Delta\epsilon_{s,max}$) and dimensionless gas solids flow-rate ratio (Π_1).

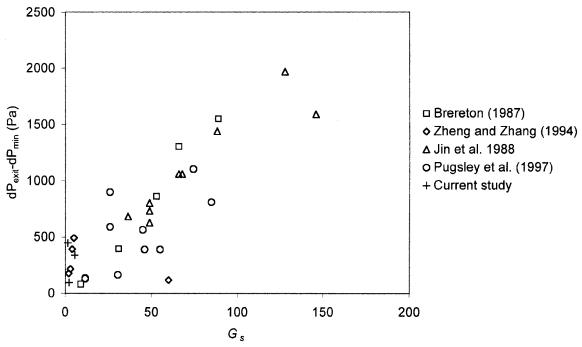

Figure 15. Maximum riser exit pressure ($dP_{exit} - dP_{min}$) and external solids circulation rate (G_s).

They illustrate the effect of the solids circulation rate on the densification of solids at the riser exit.

is the minimum pressure drop along the riser. The data presented are for abrupt exits only. Figure 15 illustrates the increase in solids densification (presented as the pressure drop) that occurs at the exit due to an increase in external solids flux.

The use of $\Delta\bar{\epsilon}_{s,\text{exit}}$ in Figure 14 and $dP_{\text{exit}} - dP_{\text{min}}$ in Figure 15, provides further evidence of the importance of CFB operating conditions on the exit effect. These results suggest that an increase in solids flux increases the refluxing of solids for a specific abrupt exit configuration. The differences between the sets of results presented in Figure 14 are probably due to the influence of particle properties and riser dimensions. An attempt to include these factors in a more detailed analysis was unsuccessful due to a lack of suitable data.

Conclusions

(1) The exit geometry in a circulating fluidized bed has a clear effect on the cross-sectional averaged solids concentration profile in a CFB riser. In a CFB combustor where the height to diameter ratio is small, this influence is important and may extend throughout the riser.

(2) The experiments reported here were performed at conditions designed to simulate the operation of a square cross-section, industrial CFB combustor. In this respect the results are novel and add to the existing knowledge based in the field.

(3) A new quantitative mechanism for solids flow at a riser exit is proposed. The mechanism explains the flow of solids in the exit bend in terms of the relative magnitude of the particle inertial and gravitational acceleration, expressed as a riser exit Froude number. The mechanism places equal emphasis on (1) solids return to the riser along the inside of the bend, and (2) the rebounding of solids from the roof of the exit returning to the riser along the outside of the exit bend.

(4) Three different quantifying measures of the influence of the riser exit are presented and used to quantify the exit effect: (1) the relative dimensionless length of influence of smooth and abrupt riser exits; (2) the exit reflection coefficient defined by Senior (1992); and (3) the relative maximum increase in solids concentration at the exit between smooth and abrupt exited risers.

(5) The dimensionless ratio (length of influence of the riser exit)/(riser height) was correlated with a comparative exit Froude number, Fr_C, based on a comparison between abrupt and smooth exits. This analysis indicated that at low values of Fr_C the length of influence of the exit (that is, the exit effect) was high. This result is consistent with the conclusions of van der Meer et al. (2000). The length of influence of the riser exit was also correlated with the riser geometry and particle properties, albeit using a restricted data set. A correlation that is a function of the gas–solid flow-rate ratio, the Reynolds, Froude and Archimedes numbers, the riser exit radius of curvature to riser diameter ratio, and the ratio of particle diameter to riser diameter is able to predict the length of influence of the exit to within 15% over a wide range of conditions.

(6) The exit Froude number, Fr_R, based on the mean solids exit velocity, was plotted against the exit reflection coefficient, R_f, defined by Senior (1992). This reflection coefficient is simply the ratio of (solids entering the bend from the riser)/(solids sent back down the riser from the bend). The correlation between R_f and Fr_R is strong, which provides further evidence that flow in the vicinity of an exit can be described by an appropriately defined Froude number. This correlation may be useful for scaling up the exit effect.

(7) For a specific riser exit configuration, the refluxing effect can be enhanced by increasing the external solids circulation rate, suggesting that operating conditions, as well as exit geometry influence the exit effect in CFB risers.

(8) It appears possible to modify the height-to-diameter ratio of academic CFB risers such that they more closely approach industrial versions without the loss of typical CFB operating conditions.

Acknowledgments

The authors are grateful for the financial support of the EPSRC in the UK.

Notation

$A_{cs,\text{core}}$ = cross-sectional area of the riser core, m^2
$A_{cs,\text{riser}}$ = cross-sectional area of the riser, m^2
A = equation coefficient
B = equation coefficient
C = equation coefficient
D = equation coefficient
a = equation coefficient
b = equation coefficient
c = equation coefficient
d = equation coefficient
e = equation coefficient
f = equation coefficient
CFBC = circulating fluidized-bed combustor
D = riser diameter, m
d_p = mean particle diameter, m
dP/dz = axial pressure gradient, Pa/m
Fr_C = comparative exit Froude number, Eq. 4
Fr_R = exit Froude number
g = acceleration due to gravity, m/s^2
G_s = superficial solids flux, kg/m$^2\cdot$s
h = distance from riser base, m
H = riser height, m
k_m = reflux ratio
LOI = axial distance where pressure profiles coincide measured in identical risers equipped with abrupt and smooth exits, m
P = pressure, Pa
dP_{exit} = pressure drop at riser exit, Pa
dP_{min} = minimum pressure drop along riser, Pa
R = radius of curvature of the riser exit, m

R_f = reflection coefficient (Senior, 1992)
R_{in} = inlet radius of curvature of the riser exit, m
R_{out} = outlet radius of curvature of the riser exit, m
U_g = superficial gas velocity, m/s
$\bar{u}_{p,dn}$ = mean downwards particle velocity (annulus), m/s
$\bar{u}_{p,up}$ = mean upwards particle velocity (core), m/s
u_{st} = mean solids velocity at the top of the riser, m/s
U_t = single-particle terminal settling velocity, m/s
$\Delta\bar{u}_{p,exit}$ = change in average exit particle velocity, m/s
Z = length of momentum exchange region (Jin et al., 1988), m
z = vertical distance, m

Greek letters

δ_f = thickness of annular film, m
ϵ = voidage fraction
$\bar{\epsilon}_{s,abrupt}$ = cross-sectional average solids concentration for abrupt exits
$\bar{\epsilon}_{s,smooth}$ = cross-sectional average solids concentration for smooth exits
$\bar{\epsilon}_s$ = cross-sectional averaged axial solids concentration
$\epsilon_{s,exit}$ = solids concentration at the exit
μ = gas viscosity, kg/ms
Π_1 = dimensionless group in Eq. 8
Π_2 = dimensionless group in Eq. 8
Π_3 = dimensionless group in Eq. 8
Π_4 = dimensionless group in Eq. 8
Π_5 = dimensionless group in Eq. 8
Π_6 = dimensionless group in Eq. 8
Π_7 = dimensionless group in Eq. 8
Π_8 = dimensionless group in Eq. 8
ρ_b = cross-sectional averaged density of solids suspension (Eq. 9)
ρ_g = gas density, kg/m^3
ρ_p = particle density, kg/m^3
Ω = LOI/H

Literature Cited

Arena, U., A. Cammarota, and L. Pistone, "High Velocity Fluidisation Behaviour of Solids in a Laboratory Scale Circulating Bed," *Circulating Fluidized Bed Technology*, P. Basu, ed., Pergamon Press, New York, p. 119–126 (1986).

Bai, D. R., Y. Jin, Z. Q. Yu, and J. Zhu, "The Axial Distribution of the Cross Sectionally Averaged Voidage in Fast Fluidized Beds," *Powder Technol.*, **71**, 51 (1992).

Bi, H. T., J. Zhou, S.-Z. Qin, and J. R. Grace, "Annular Wall Layer Thickness in Circulating Fluidized Bed Risers," *Can. J. Chem. Eng.*, **74**, 811 (1996).

Brereton, C., "Fluid Mechanics of High Velocity Fluidized Beds," PhD Diss., Univ. of British Columbia, Vancouver, Canada (1987).

Brereton, C. M. H., and J. R. Grace, "End Effects in Circulating Fluidized Bed Hydrodynamics," *Circulating Fluidized Bed Technology IV*, A. A. Avidan, ed., Hidden Valley, PA, p. 137–144 (1994).

Glicksman, L. R., "Heat Transfer in Circulating Fluidised Beds," *Circulating Fluidised Beds*, J. R. Grace, A. A. Avidan, and T. M. Knowlton, eds., Chapman and Hall, London, pp. 261–311 (1997).

Grace, J. R., "High Velocity Fluidized Bed Reactors," *Chem. Eng. Sci.*, **45**(8), 1953 (1990).

Harris, B. J., "The Hydrodynamics of Circulating Fluidized Beds," PhD Thesis, Univ. of Cambridge, Cambridge, UK (1993).

Harris, A. T., R. B. Thorpe, and J. F. Davidson, "The Prediction of Particle Cluster Properties in the Near Wall Region of a Vertical Riser," *Powder Technol.*, **127**, 128 (2002).

Horio, M., "Hydrodynamics," *Circulating Fluidized Beds*, Chap. 2, J. R. Grace, A. A. Avidan, and T. M. Knowlton, eds., Chapman & Hall, London, p. 21 (1997).

Jin, Y., Z. Yu, C. Qi, and D. Bai, "The Influence of Exit Structures on the Axial Distribution of Voidage in a Fast Fluidized Bed," *Fluidization 88 Science and Technology, The Third China-Japan Symposium*, M. Kwauk and D. Kunii, eds., Science Press, Beijing, 165 (1988).

Jin, Y., J. Zhu, and Z. Yu, "Hydrodynamics," *Circulating Fluidized Beds*, Chap. 16, J. R. Grace, A. A. Avidan, and T. M. Knowlton, eds., Chapman & Hall, London, p. 21 (1997).

Johnsson, F., A. Vrager, and B. Leckner, "Solids Flow Pattern in the Exit Region of a CFB-Furnace-Influence of Exit Geometry," *15th Int. Conf. on Fluidized Bed Combust*., Savannah, GA, ASME (1999).

Lim, K. S., J. X. Zhu, and J. R. Grace, "Hydrodynamics of Gas-Solid Fluidization," *Int. J. Multiphase Flow*, **21**(Suppl.), 141 (1995).

Martin, M. P., C. Derouin, P. Turlier, M. Forissier, G. Wild, and J. R. Bernard, "Catalytic Cracking in Riser Reactors," *Chem. Eng. Sci.*, **47**(9–11), 2319 (1992a).

Martin, M. P., P. Turlier, G. Wild, and J. R. Bernard, "Gas and Solid Behaviour in Cracking Circulating Fluidized Beds," *Powder Technol.*, **70**, 249 (1992b).

Mickal, V., P. Schausberger, F. Winter, H. Hofbauer, C. Brunner, and A. Aichernig, "Effect of Exit Geometry on the Solids Distribution in a CFB Reactor for the Fluidization of Fine Particles: Determination on Internal Back-Mixing with Semi-Theoretical Modelling," *Fluidisation X*, Engineering Foundation, New York, p. 245 (2001).

Pugsley, T., D. Lapointe, B. Hirschberg, and J. Werther, "Exit Effects in Circulating Fluidized Bed Risers," *Can. J. Chem. Eng.*, **75**, 1001 (1997).

Senior, R. C., "Circulating Fluidized Bed Fluid and Particle Mechanics: Modelling and Experimental Studies with Application to Combustion," PhD Thesis, Univ. of British Columbia, Vancouver, Canada (1992).

van der Meer, E. H., R. B. Thorpe, and J. F. Davidson, "Flow Patterns in the Square Cross-Section Riser of a Circulating Fluidized Bed and the Effect of Riser Exit Design," *Chem. Eng. Sci.*, **55**, 4079 (2000).

van der Meer, E. H., "Riser Exits and Scaling of Circulating Fluidized Beds," PhD Diss., Univ. of Cambridge, Cambridge, UK (1997).

Werther, J., and B. Hirschberg, "Solids Motion and Mixing," *Circulating Fluidized Beds*, Chap. 4, J. R. Grace, A. A. Avidan, and T. M. Knowlton, ed., Chapman & Hall, London, p. 119 (1997).

Zheng, Q., and H. Zhang, "Experimental Study of the Effect of Bed Exits with Different Geometric Structure on Internal Recycling of Bed Material in CFB Boilers," *Circulating Fluidized Bed Technology IV*, A. A. Avidan, ed., Hidden Valley, PA, p. 145–151 (1994).

Manuscript received June 11, 2001, and revision received July 3, 2002.